

# Runoff Coefficients of High-flow Events in Undisturbed New England Basins

Iman Hosseini-Shakib<sup>1</sup>, Kevin Gardner<sup>2</sup>, and Anne Lightbody<sup>3</sup>

<sup>1</sup>Research Assistant at Department of Civil and Environmental Engineering, University of New Hampshire, Durham NH 03824, USA

<sup>2</sup>Professor at Department of Civil and Environmental Engineering, University of New Hampshire, Durham NH 03824, USA

<sup>3</sup>Associate Professor at Department of Earth Sciences, University of New Hampshire, Durham NH 03824, USA

November 23, 2022

## Abstract

The New England region in the Northeast U.S. receives high annual precipitation as rain and snow, which results in floods that endanger people and infrastructure. Owing to the complexity of hydrologic systems, increases in the frequency and intensity of large precipitation events do not always translate into increases in surface runoff measured as event flow at the basin outlet. However, recent studies have recognized positive trends in the frequency and magnitude of high-flow events in New England. For high-flow events of equal or greater than 2-year daily runoff, the runoff coefficients, or the fraction of precipitation converted into surface runoff during an event, were determined for 28 undisturbed New England basins with natural flow conditions. Results indicated that runoff coefficients increase in magnitude and variability with distance from the Atlantic coast toward the north and west. The average runoff coefficient of high-flow events across all basins is 0.90, while there exist many high-flow events with runoff coefficients greater than one. Also, runoff coefficients were generally stationary showing that flood events in undisturbed basins have remained proportional to precipitation inputs, despite increases in extreme precipitation, possibly due to shifts in evapotranspiration, snowpack, and soil moisture. Flood management efforts should continue to focus on large springtime precipitation events, which generate the highest runoff coefficients. Finally, this study can serve as a reference point for future exploration of the flood susceptibility of basins with anthropogenic alterations like dam construction or land use change.

# Runoff Coefficients of High-flow Events in Undisturbed New England Basins

I. Hosseini-Shakib<sup>1</sup>, K. H. Gardner<sup>1</sup>, and A. F. Lightbody<sup>2</sup>

<sup>1</sup>Department of Civil and Environmental Engineering, University of New Hampshire, Durham NH 03824, USA

<sup>2</sup>Department of Earth Sciences, University of New Hampshire, Durham NH 03824, USA

Corresponding author: Iman Hosseini-Shakib ([ih1@wildcats.unh.edu](mailto:ih1@wildcats.unh.edu))

## Key Points:

- Many high-flow events in New England produce runoff coefficients greater than 1.0, indicating that more water was produced than could be attributed to event flow from recent precipitation.
- Runoff coefficients of high-flow events in New England generally increase in magnitude and variability with distance from the coast toward the north and west.
- Since 1981, the runoff coefficients of high-flow events at 25 of 28 stations were stationary, suggesting that recent climate change has not significantly impacted flood-generating mechanisms in undisturbed New England basins with natural flow.

## Abstract

The New England region in the Northeast U.S. receives high annual precipitation as rain and snow, which results in floods that endanger people and infrastructure. Owing to the complexity of hydrologic systems, increases in the frequency and intensity of large precipitation events do not always translate into increases in surface runoff measured as event flow at the basin outlet. However, recent studies have recognized positive trends in the frequency and magnitude of high-flow events in New England. For high-flow events of equal or greater than 2-year daily runoff, the runoff coefficients, or the fraction of precipitation converted into surface runoff during an event, were determined for 28 undisturbed New England basins with natural flow conditions. Results indicated that runoff coefficients increase in magnitude and variability with distance from the Atlantic coast toward the north and west. The average runoff coefficient of high-flow events across all basins is 0.90, while there exist many high-flow events with runoff coefficients greater than one. Also, runoff coefficients were generally stationary showing that flood events in undisturbed basins have remained proportional to precipitation inputs, despite increases in extreme precipitation, possibly due to shifts in evapotranspiration, snowpack, and soil moisture. Flood management efforts should continue to focus on large springtime precipitation events, which generate the highest runoff coefficients. Finally, this study can serve as a reference point for future exploration of the flood susceptibility of basins with anthropogenic alterations like dam construction or land use change.

## Plain Language Summary

This is a study on New England floods from 1981 to 2016 to see if climate change has had considerable impacts on the causes of flooding; that is, rainfall, snowmelt, soil moisture, etc. To do this, the percentage of rainfall that runs off the land and creates flooding has been analyzed in regions of no human disturbance in nature such as dam or urban construction like buildings and pavement. Our results show that, in spite of changing climate and increasing rainfalls, the percentage of rainfall that runs off the land during floods in these regions is not a lot different from around 40 years ago.

## 1 Introduction

The New England region in the Northeast U.S. receives high annual precipitation as rain and snow, which results in floods that endanger people and infrastructure (Smith et al., 2019). Moreover, the threat of flood-related dam failure poses additional risk to human lives (National Weather Service, 2018). Floods are particularly frequent during intense rainfall and high snow melt, especially when the ground is frozen or saturated (Paulson et al., 1991). Regional climate change is expected to change precipitation patterns and increase precipitation intensity, creating concern about increasing flood levels and resulting threats to dams and other infrastructure systems (Matthews et al., 2011). Ongoing land use change, especially urbanization, is also expected to change flood risks (Satterthwaite, 2008). To isolate the potential impact of climate change on basin response to precipitation events, this paper investigates the relationship between precipitation and runoff generation across New England at locations where minimal development has taken place.

### 1.1 Historical Trends in Precipitation and Runoff

Since 1901, annual precipitation and extreme precipitation events have increased in both intensity and frequency in the U.S., with the largest increases in the Northeast (Wuebbles et al., 2017). Many studies confirm positive trends in the intensity and frequency of extreme precipitation events, especially in recent decades (Demaria et al., 2016; Groisman et al., 2005, 2004; Karl and Knight,

1998; Madsen and Figdor, 2007; Mallakpour and Villarini, 2017; Spierre et al., 2010). In addition, increases have been largest during spring and fall (Spierre et al., 2010).

Floods have also increased in recent years in New England, though the trends are more complicated. Ordinarily, precipitation leads to event flow, which is a short-term increase in river discharge above base flow. However, owing to the complexity of hydrologic systems, increases in the frequency and intensity of large precipitation events do not always translate into increases in surface runoff measured as event flow at the basin outlet (Berghuijs et al., 2016). A recent study found upward trends (mainly a step increase around 1970) in 25 out of 28 gauge stations in New England watersheds with natural or near-natural flood generating conditions, i.e., basins without significant human alteration (Collins, 2009). Similarly, Hodgkins and Dudley (2005) found significant increases in March mean flows in northern New England, and McCabe and Wolock (2002) found a step increase in daily streamflow around 1970 across the conterminous U.S. Slater and Villarini (2016) attributed observed increases in flood risk patterns in the Northeast U.S. to changes in basin wetness and water storage, while Collins (2019) identified changing flood generation mechanisms as contributing to the increasing frequency of warm-season (June – October) floods in New England. Other recent studies have also shown positive trends in high flows in the Northeast U.S. (Arnell and Gosling, 2016; Demaria et al., 2016; Ivancic and Shaw, 2015; Prosdocimi et al., 2015).

However, some studies could not confirm the existence of increasing trends in high flows in New England. A study of nine gauges in New England prior to 1997 found increasing precipitation but no change in high-flow magnitude (Small et al., 2006). Another study of 435 gauges (19 in New England) prior to 1999 also found increases in precipitation but detected no change in the timing of flow characteristics on a monthly time scale, likely because precipitation increases were concentrated in the autumn but high flows occurred in spring (Lins and Slack, 2005). In fact, seasonality is often critical to flood frequencies because soil moisture, snow melt, and evapotranspiration vary over the course of the year, so the timing of large precipitation events affects the amount of flow generated. In addition, recent increases in precipitation may have been offset by increases in temperature, which decrease the snow pack and increase evapotranspiration (Ivancic and Shaw, 2015). Thus, there is still some uncertainty in recent historical changes in flood flows in New England, let alone difficulty in predicting future changes. The analysis of trends in peak flows is complicated by the fact that each precipitation event introduces a different amount of water into the drainage basin.

## 1.2 Future Flood Frequencies

New England is expected to get wetter in the future: climate model projections up to 2100 show more frequent and larger precipitation events along with more accentuated seasonal variability of precipitation (Hirsch and Archfield, 2015; Mallakpour and Villarini, 2017). Projections reveal that many parts of the country, including New England, that now receive the bulk of their wintertime precipitation as snow will start to receive increasing amounts of wintertime rain, resulting in consequent decreases in the amount of snowpack and snowmelt (Easterling et al., 2017). Therefore, increases in the frequency and magnitude of large precipitation events will likely continue.

Several studies have used detailed rainfall-runoff modeling to predict future flood recurrence intervals in the face of climate change. For example, a macro-scale hydrologic model for the Upper Midwest driven with projected future climate scenarios anticipated a 10% to 30% increase in the magnitude of 100-year floods by the 2080s (Byun et al., 2019). Such detailed modeling approaches

can take into account differences in antecedent soil moisture and snow pack, which can lead to differences in flood response for a single basin (Woldemeskel and Sharma, 2016). However, detailed numerical models require a large investment of time and resources, which impedes their rapid deployment for management decisions related to flood risk.

Another simpler approach is to rely on the runoff coefficient (RC), which is the ratio of event flow to precipitation. Because it normalizes for water input magnitude, the RC is a useful tool for comparing different years, basins, seasons, and events. The applicability of RCs in hydrological studies is widely accepted based on a long history of study and use. For instance, a study of 21 basins in MA revealed some consistency in RCs for unregulated basins (Colonell and Higgins, 1973). RCs were also found useful in the estimation of peak flows in basins from NH to SC (Hewlett et al., 1977) and from NY to AL (Woodruff and Hewlett, 1970).

However, even though numerous studies have suggested that precipitation and flood events have both recently increased in magnitude in New England, few studies have evaluated whether these changes are proportional, and therefore whether there have been observable changes in RCs.

In addition, because future increases in precipitation are a key factor in future flood risk, RCs may be useful clues to future flood recurrence intervals resulting from changes in input precipitation, at least under conditions during which flood-generation mechanisms remain similar to current conditions. Therefore, investigating long-term temporal and spatial trends in RC in New England is a useful first step in assessing future increases in vulnerability to floods.

#### 1.4 Study Goals

This study investigates the annual, seasonal and spatial variations of RCs in New England for high-flow events using recent long-term precipitation and runoff data in non-human-impacted basins. The objective of this analysis is to understand the extent to which changing patterns in precipitation influence the magnitude and frequency of high-flow events.

## 2 Methods

### 2.1 Gauge Selection and Input Data Processing

This study focused on 28 long-term streamflow gauge stations (Figure 1, Table 1). All study gauges were included in the New England Hydro-Climatic Data Network (HCDN), which is a subset of U.S. Geological Survey (USGS) gauges that were screened for natural, or near-natural, flood-generating conditions that have not changed over the period of record. In addition, this set of gauges had been previously used for runoff trend analysis (Collins, 2009). Gauges in undisturbed watersheds were selected to focus on climatic rather than local anthropogenic factors, such as large dams and changes in land use. Time series of daily flow data (1981-2016) at each station (USGS, 2019) were formed in R using the waterData Package (Ryberg and Vecchia, 2017). The time period of study was chosen to be long enough (36 years) to average over decadal-scale climate variability, to be recent enough to overlap with the availability of high-resolution gridded daily precipitation data (see below), and to occur since 1975, which is approximately when potential step changes in streamflow and floods occurred in the Northeast U.S. (Armstrong et al., 2014, 2012; Collins, 2009; McCabe and Wolock, 2002) and warming due to radiative forcing associated with greenhouse gasses started to emerge from the noise of natural variability (Hansen et al., 2010).

The drainage basin for each streamflow gauge was delineated using the USGS StreamStats application (USGS, 2017), which is based on 10-m resolution digital elevation models of the region.

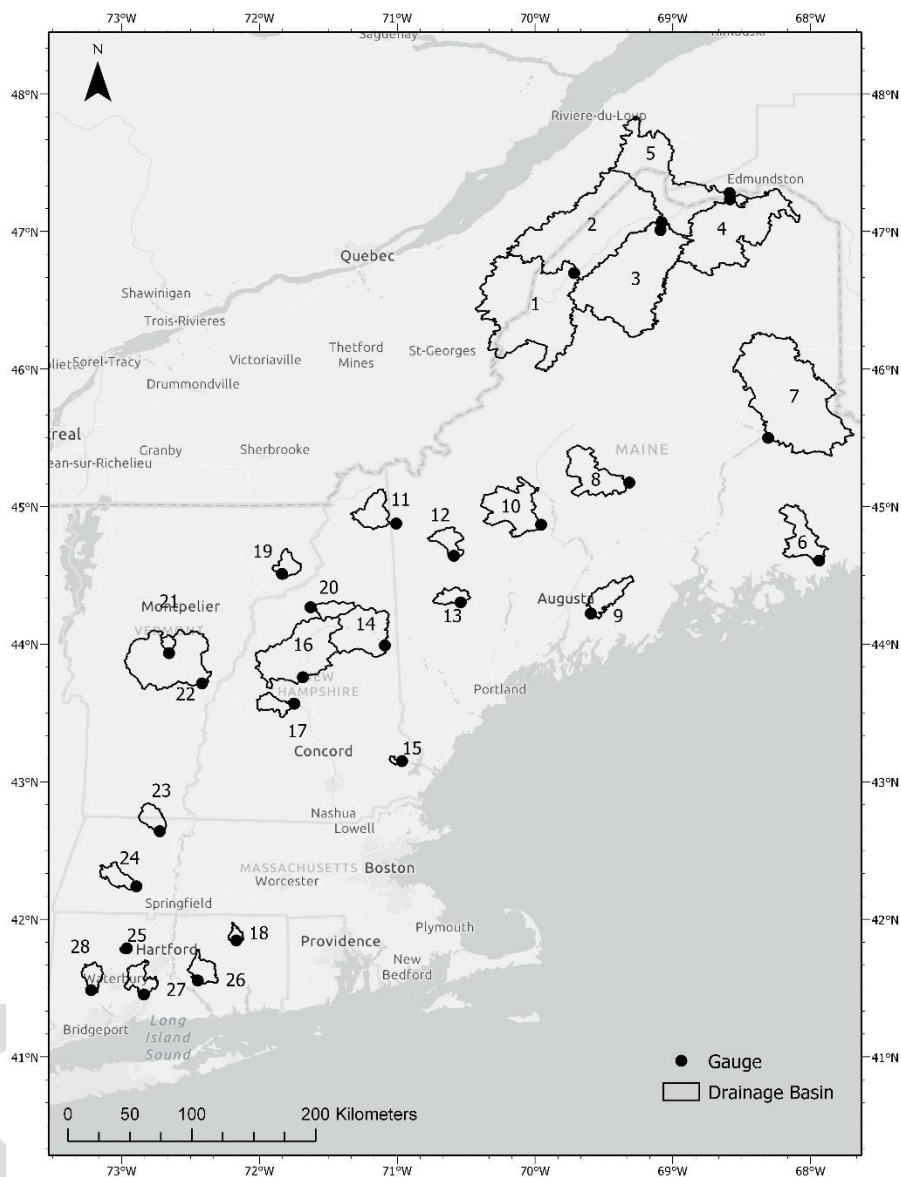


**Figure 1.** Selected streamflow gauges and drainage basins. Numbers correspond to basin numbering scheme shown in Table 1.

**Table 1.** Selected New England streamflow gauges, gauge altitude, and drainage basin size.

| No. | USGS Gauge Station ID | USGS Gauge Station Name                      | State | Latitude | Longitude | Altitude (m) | Drainage Area (sq. km.) |
|-----|-----------------------|--|-------|----------|-----------|--------------|-------------------------|
| 1   | 01010000              | St. John River at Ninemile Bridge            | ME    | 46.7006  | -69.7156  | 283.8        | 3473                    |
| 2   | 01010500              | St. John River at Dickey                     | ME    | 47.0131  | -69.0881  | 179.9        | 6941                    |
| 3   | 01011000              | Allagash River near Allagash                 | ME    | 47.0697  | -69.0794  | 184.3        | 3828                    |
| 4   | 01013500              | Fish River near Fort Kent                    | ME    | 47.2375  | -68.5828  | 155.9        | 2261                    |
| 5   | 01014000              | St. John River below Fish River at Fort Kent | ME    | 47.2833  | -68.5853  | 153.9        | 15317                   |
| 6   | 01022500              | Narraguagus River at Cherryfield             | ME    | 44.6081  | -67.9353  | 13.5         | 588                     |
| 7   | 01030500              | Mattawamkeag River near Mattawamkeag         | ME    | 45.5011  | -68.3058  | 66.1         | 3673                    |
| 8   | 01031500              | Piscataquis River near Dover-Foxcroft        | ME    | 45.1750  | -69.3147  | 109.3        | 772                     |
| 9   | 01038000              | Sheepscot River at North Whitefield          | ME    | 44.2228  | -69.5939  | 30.8         | 376                     |
| 10  | 01047000              | Carrabassett River near North Anson          | ME    | 44.8692  | -69.9550  | 92.4         | 914                     |
| 11  | 01052500              | Diamond River near Wentworth Location        | NH    | 44.8775  | -71.0075  | 383.9        | 394                     |
| 12  | 01055000              | Swift River near Roxbury                     | ME    | 44.6428  | -70.5889  | 187.7        | 251                     |
| 13  | 01057000              | Little Androscoggin River near South Paris   | ME    | 44.3039  | -70.5397  | 136.2        | 190                     |
| 14  | 01064500              | Saco River near Conway                       | NH    | 43.9908  | -71.0906  | 127.5        | 997                     |
| 15  | 01073000              | Oyster River near Durham                     | NH    | 43.1486  | -70.9656  | 19.9         | 31.5                    |
| 16  | 01076500              | Pemigewasset River at Plymouth               | NH    | 43.7592  | -71.6861  | 139.3        | 1611                    |
| 17  | 01078000              | Smith River near Bristol                     | NH    | 43.5664  | -71.7483  | 137.1        | 222                     |
| 18  | 01121000              | Mount Hope River near Warrentonville         | CT    | 41.8436  | -72.1694  | 102.0        | 74                      |
| 19  | 01134500              | Moose River at Victory                       | VT    | 44.5117  | -71.8378  | 336.5        | 195                     |
| 20  | 01137500              | Ammonoosuc River at Bethlehem Junction       | NH    | 44.2686  | -71.6308  | 359.9        | 227                     |
| 21  | 01142500              | Ayers Brook at Randolph                      | VT    | 43.9344  | -72.6583  | 192.2        | 79                      |
| 22  | 01144000              | White River at West Hartford                 | VT    | 43.7142  | -72.4186  | 114.2        | 1787                    |
| 23  | 01169000              | North River at Shattuckville                 | MA    | 42.6383  | -72.7256  | 140.5        | 231                     |
| 24  | 01181000              | West Branch Westfield River at Huntington    | MA    | 42.2372  | -72.8961  | 118.4        | 244                     |
| 25  | 01188000              | Burlington Brook near Burlington             | CT    | 41.7861  | -72.9653  | 217.6        | 10.6                    |
| 26  | 01193500              | Salmon River near East Hampton               | CT    | 41.5522  | -72.4497  | 19.6         | 259                     |
| 27  | 01196500              | Quinnipiac River at Wallingford              | CT    | 41.4503  | -72.8413  | 5.9          | 298                     |
| 28  | 01204000              | Pomperaug River at Southbury                 | CT    | 41.4819  | -73.2246  | 50.5         | 195                     |

For precipitation data, the PRISM (Parameter-elevation Regression on Independent Slopes Model) 2.5 arcmin (~4-km) resolution daily gridded data for the U.S. were used from 1981 to 2016 (PRISM Climate Group, 2004). The gridded precipitation data were clipped to each basin in R using basin boundary shapefiles. Grid cell values were then averaged for each day within each basin to obtain the mean daily precipitation. The drainage basins for three of the stations (Station 1; St. John River at Ninemile Bridge, Station 2; St. John River at Dickey, and Station 5; St. John River below Fish River at Fort Kent) crossed the international border into Canada, where PRISM data were unavailable. For each of these basins, the average daily precipitation for the U.S. portion of the watershed was used to represent the average daily precipitation of the entire basin.

## 2.2 High-flow Event Definition and Runoff Coefficient Calculation

High-flow events were defined using a peak-over-threshold method to be all large events that yielded a maximum daily discharge equal to or greater than a basin-specific threshold discharge value. Threshold discharge values for each basin were determined based on the recurrence interval of various daily flows. Nominal flood frequency magnitudes for 2-year, 5-year, and 10-year floods at the stations (basin outlets) were obtained using USGS daily flow data (1981-2016), with analysis performed in R (R Core Team, 2019) using a generalized extreme value (GEV) distribution function within the Extreme Value Analysis (extRemes) package (Gilleland and Katz, 2016). A sensitivity analysis (see below) was performed to determine the impact of the high-flow event threshold choice.

Hydrograph separation for each high-flow event was performed to separate event flow from base flow (Figure 2). First, the beginning and end of the event were determined. Many high-flow events were preceded and/or followed by one or more smaller hydrograph peaks, especially during spring, resulting in a prolonged departure of measured discharge from seasonal baseflow. To select the beginning and end of the event, we used  $n$ -day local minima for both sides. That is, the beginning was defined to be the first day before the event peak that had a discharge that was equal to or smaller than the flow of the previous  $n - 1$  days. Likewise, the end was defined to be the first day after the event peak that had a discharge that was equal to or smaller than the flow of the next  $n - 1$  days. A sensitivity analysis (see below) was performed to determine the impact of the length  $n$ .

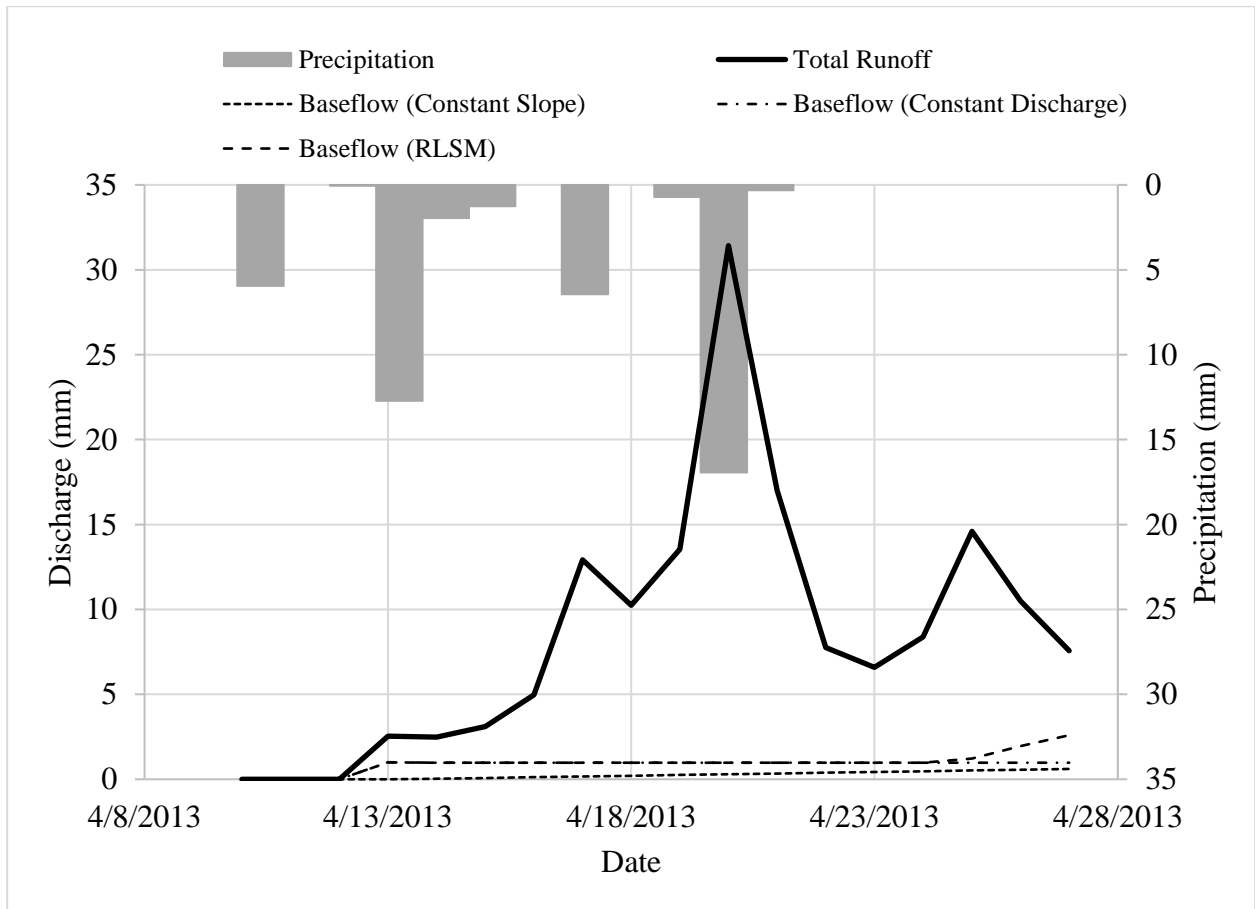
Once the event hydrograph was determined, baseflow was separated using one of four different methods. First, for comparison purposes, baseflow during the event was assumed to be negligible and no baseflow separation was performed. Second, for the constant discharge method, baseflow throughout the event was assumed to equal the discharge at the event beginning. Third, for the constant slope method, baseflow during the event was assumed to increase at a rate of  $0.000546 \text{ m}^3 \text{ s}^{-1} \text{ km}^{-2} \text{ h}^{-1}$  (Dingman, 2002). Fourth, baseflow during the event was estimated using the RHydro package (Reusser et al., 2017) using the re-scaled LOWESS-smoothed window minima (RLSM) which uses the Locally Weighted Scatterplot Smoothing (LOWESS) method (Cleveland, 1979) to smooth the local minima as baseflow values. The RLSM method was applied in its default format with the LOWESS smoother span set to 0.1. For each method, once baseflow was determined, it was subtracted from measured discharge, and the resulting event flow was integrated over the entire event to determine total event discharge. Total event discharge was divided by basin area to obtain total event runoff. A sensitivity analysis (see below) was performed to determine the impact of baseflow separation method.

Total event precipitation was determined by summing the corresponding basin hyetograph for the event. The time window for summation started one concentration time before the beginning of the discharge event and ended one concentration time before the end of the discharge event. Determination of the concentration time for each basin based on the historical hyetograph and hydrograph was performed in R using the RHydro package (Reusser et al., 2017).

Finally, the RC for each high-flow event was obtained by dividing total event runoff (following hydrograph separation) by total event precipitation.



211



212

213 **Figure 2.** Sample flood of April 2013 at Diamond River near Wentworth Location comparing  
 214 different baseflow separation methods: constant discharge, constant slope, and re-scaled LOW-  
 215 ESS-smoothed window minima (RLSM).

### 216 2.3 Statistical and Sensitivity Analysis

217 Trend analysis was conducted using the non-parametric Mann-Kendall method which performs  
 218 a monotonic trend test (e.g., Hipel and McLeod, 1994). The “Kendall” package in R (McLeod,  
 219 2011) was used to perform trend analysis in this study. Correlations were assessed using a Pearson  
 220 linear correlation coefficient. For all statistical analyses, significance was assessed at the 90% con-  
 221 fidence level for  $N = 28$  independent observations.

222 To explore the robustness of results, a sensitivity analysis was conducted on the following three  
 223 calculation attributes:

- 224 • A: different recurrence interval for the high-flow event threshold,
- 225 • B: different duration of local minima used in determining the beginning and end of each
- 226 event, and
- 227 • C: different baseflow separation methods.

228 Table 2 presents the various alternatives for each of these attributes and identifies the base alter-  
 229 native for each. When comparing alternatives for one attribute, the other attributes were set to their

base alternatives. For example, for scenario B1, the local minima duration was set to 3 days, while the high-flow event threshold was retained at its base alternative (2-year flood) and the baseflow separation method was also retained at its base alternative (RLSM method). Below, the term “base scenario” is used when each of the attributes is set to its base alternative (e.g., scenario A1, B2, or C4, which are all equivalent).

**Table 2.** Attributes and alternatives used in sensitivity analysis, including the base alternative for each attribute.

| Attribute |                           | Alternative |                     |
|-----------|---------------------------|-------------|---------------------|
| A         | High-flow Event Threshold | A1          | 2-yr Flood (base)   |
|           |                           | A2          | 5-yr Flood          |
|           |                           | A3          | 10-yr Flood         |
| B         | Local Minima Duration     | B1          | 3-day Minima        |
|           |                           | B2          | 5-day Minima (base) |
|           |                           | B3          | 7-day Minima        |
| C         | Baseflow Separation       | C1          | No Separation       |
|           |                           | C2          | Constant Discharge  |
|           |                           | C3          | Constant Slope      |
|           |                           | C4          | RLSM (base)         |

### 3 Results and Discussion

#### 3.1 High-Flow Events

A total of 696 high-flow events (nominal 2-year return period or greater) were identified during the study period (1981-2016) in the 28 study basins. Many high-flow events were regional in scope, affecting the majority of the study basins. Some high-flow events, however, were more localized and only observed at a few gauges.

Observed flood recurrence intervals did not exactly match the nominal recurrence interval, especially for the high-frequency 2-year return period: 696 high-flow events divided by 36 years divided by 28 study basins results in an average frequency of 0.69, rather than 0.5 as would be expected for a 2-year return period. The difference was smaller for the 5-year return period (235 events, average frequency of 0.23) and the 10-year return period (104 events, average frequency of 0.10), and likely results from the use of a distribution function to calculate nominal recurrence intervals for frequent events. However, as discussed below, the high-flow event threshold attribute had a relatively small effect on the magnitude and trend of calculated RCs, and uncertainty in the exact flood magnitudes likely had an even smaller impact.

#### 3.2 Runoff Coefficient Magnitude

Across all 28 basins, the average RC for high-flow events in New England was close to and in some cases greater than 1.0 (Table 3). The highest RC of a high-flow event was 6.86, which occurred in the drainage basin of Station 1, St. John River at Ninemile Bridge in April 26, 2001. In total, twenty events exhibited RCs that exceeded a value of 3.0 (Table 3). Moreover, 9 out of 28 basins (32%) have average RCs greater than 1.0 during high-flow events (Table 4), when RCs are calculated using the base scenario. Among all the high-flow events, 511 (73%) show RC less than

1.0 showing the prevalence of precipitation as the main runoff generating mechanism. Although with different metrics, Collins et al. (2014) report roughly the same proportion of all floods (74%) that are attributed solely to rain. To check for the impact of outlier events on the basins with high average RC magnitudes, medians were also calculated and compared to the averages. Results show that medians and averages follow a similar pattern and there is no basin with a large difference between average and median (Table 4) implying insignificant impact of outlier events on average RCs.

The prevalence of basins with high RC, and individual events with RCs greater than 1.0, indicates the substantial role of snow-dependent flood generation mechanisms, including snowmelt or rain-on-snow, in regional high-flow events. This is in strong contrast to events in lower latitudes. For instance, average RCs for the five Connecticut River basins ranged from 0.53 to 0.68. In the following discussion, we focus on the average RC for each basin, rather than the most extreme RCs observed, to average across different antecedent soil moisture conditions, which can strongly affect the RC for an individual basin (Woldemeskel and Sharma, 2016).

**Table 3.** Twenty largest runoff coefficients calculated using the base scenario observed in study basins

| No. | Runoff Coefficient | Station | Date Hydrograph Peaked | No. | Runoff Coefficient | Station | Date Hydrograph Peaked |
|-----|--------------------|---------|------------------------|-----|--------------------|---------|------------------------|
| 1   | 6.86               | 1       | 4/26/2001              | 11  | 3.24               | 11      | 3/31/1998              |
| 2   | 6.52               | 2       | 4/26/2001              | 12  | 3.23               | 11      | 4/9/1991               |
| 3   | 4.25               | 23      | 4/18/1982              | 13  | 3.23               | 19      | 4/19/1982              |
| 4   | 4.16               | 22      | 4/24/2001              | 14  | 3.16               | 10      | 3/31/1998              |
| 5   | 3.90               | 11      | 4/23/1992              | 15  | 3.09               | 19      | 3/31/1986              |
| 6   | 3.74               | 12      | 1/20/1996              | 16  | 3.07               | 11      | 4/28/1994              |
| 7   | 3.73               | 5       | 4/25/2008              | 17  | 3.07               | 2       | 4/29/1982              |
| 8   | 3.58               | 19      | 4/25/2001              | 18  | 3.06               | 20      | 4/27/1982              |
| 9   | 3.40               | 17      | 4/24/2001              | 19  | 3.06               | 23      | 3/31/1987              |
| 10  | 3.24               | 22      | 4/18/1982              | 20  | 3.06               | 22      | 3/31/1987              |

The exact magnitude of the RC within each basin depended on the details of how it was calculated. Figure 3 shows the sensitivity of the average RC for each basin to different calculation attributes. With respect to the high-flow event threshold, the 2-yr (A1 scenario) flood was chosen as the base scenario (in order to retain the greatest number of events), resulting in an average runoff coefficient of 0.90 across all basins. Increasing the threshold to a 5-yr flood (A2) decreased the average RC by 1%, while increasing the threshold to the 10-yr flood (A3) decreased the average RC by 3%. However, different basins exhibited different responses to changes in the high-flow event threshold (Figure 3a). For example, Stations 2 and 5 exhibited the largest RCs for scenario A1, Stations 1 and 22 exhibited the largest RCs for scenario A2, and Stations 13 and 25 exhibited the largest RCs for scenario A3. This can be explained by differences in flood-generating mechanisms for each basin.

On the other hand, the other two calculation attributes, local minima duration and baseflow separation method, had slightly greater impacts on average RC magnitudes, but responses were relatively consistent among all basins. That is, compared to the baseline scenario (5-day minima; B2), selection of 3-day minima (B1) would on average increase the RC magnitude by 5%, and a small increase was observed for most stations (Figure 3b). Likewise, selection of 7-day minima (B3) would on average decrease the RC magnitude by 12%, and a small decrease was observed for most stations.

The choice of baseflow separation method (C) caused the largest changes in RC magnitude, but again changes were relatively similar among basins. Compared to the baseline scenario (RLSM method; C4), selection of no baseflow separation (C1), the constant discharge method (C2), and the constant slope method (C3) resulted in 71%, 48%, and 20% increase in average RC, respectively (Figure 3c). No baseflow separation (C1) resulted in the largest RCs because it included all discharge during the event. The constant discharge method (C2) resulted in the second highest RCs because it did not take into account the typical increase in baseflow that occurs during a water input event (Dingman, 2002). It is unclear why the constant slope method uniformly resulted in higher RCs than the RLSM method, because both of these methods accounted for a gradual rise in baseflow during the high-flow event; it is possible that the value of the constant slope increase was too gradual to account for baseflow increases in New England. Regardless, adopting the RLSM method as the base scenario is most conservative and results in the lowest reported RCs.

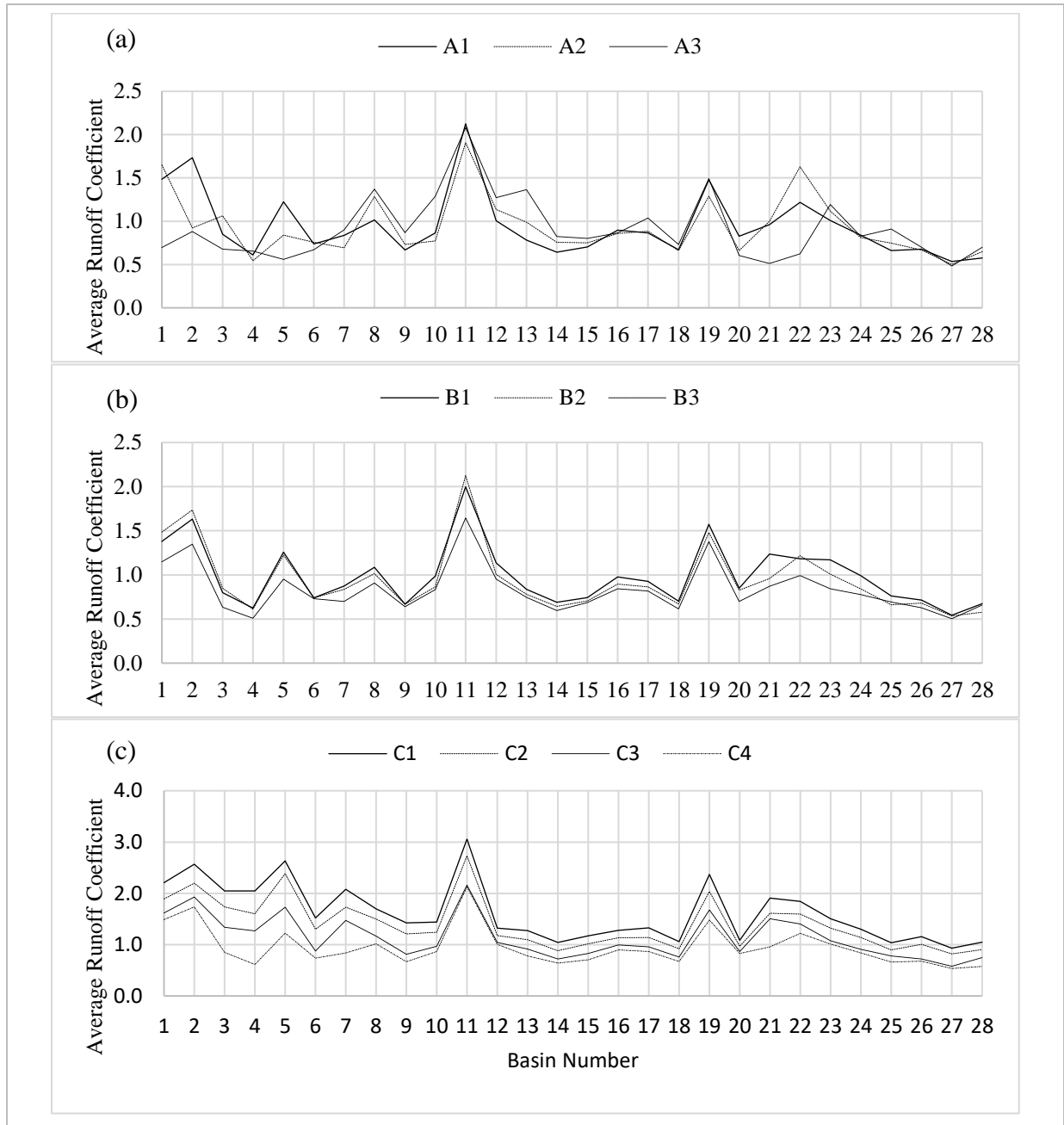


**Figure 3.** Sensitivity of average runoff coefficient to (a) high-flow events to high-flow event threshold, (b) local minima duration, and (c) baseflow separation method.

### 3.2 Spatial Variability of RCs

Different basins were differently prone to flooding. For the base scenario, the minimum average RC was 0.53 at the drainage basin of Station 27 (Quinnipiac River at Wallingford, CT) while the maximum was 2.12 at the drainage basin of Station 11 (Diamond River near Wentworth Location, NH). Thus, there was a four-fold difference in average RCs during high-flow events. Moreover,

observed differences in RCs between gauges were greater than differences due to calculation alternatives (Figure 3). A weak relationship was observed between basin size and average RC ( $p = 0.096$ ), consistent with basin size driving dominant runoff mechanisms. It is also possible that daily gridded precipitation data limited the estimation of RCs, particularly in smaller basins.

Figure 4 shows the geographical distribution of average RC in New England for the base scenario, which reveals that the average RC generally increases northwest away from the coast. In fact, significant linear positive relationships were present between gauge altitude and average RC ( $r^2 = 0.44$ ,  $p = 0.0001$ ) as well as gauge latitude and average RC ( $r^2 = 0.22$ ,  $p = 0.01$ ), both of which are related to the fraction of annual precipitation that falls as snow. These relationships are consistent with previous observations that, although precipitation is the major source of New England floods, the role of rain-on-snow and snowmelt driven events is accentuated with distance from the coast, as well as increasing altitude and latitude (Collins et al., 2014). As shown in Figure 5, the standard deviation of RCs similarly increases with distance northwest from the coast. Significant linear positive relationships were present between gauge altitude and RC standard deviation ( $r^2 = 0.35$ ,  $p = 0.0008$ ) as well as gauge latitude and RC standard deviation ( $r^2 = 0.35$ ,  $p = 0.0008$ ), as well as between gauge altitude and RC standard deviation as a fraction of average RC ( $r^2 = 0.18$ ,  $p = 0.025$ ) as well as gauge latitude and RC standard deviation as a fraction of average RC ( $r^2 = 0.38$ ,  $p = 0.0004$ ). In other words, greater RC variability accompanied greater average RC ( $r^2 = 0.73$ ,  $p < 0.0001$ ), but RC variability as a fraction of average RC also exhibited substantial differences, perhaps because of the variability in runoff-generation mechanisms in snowier basins.

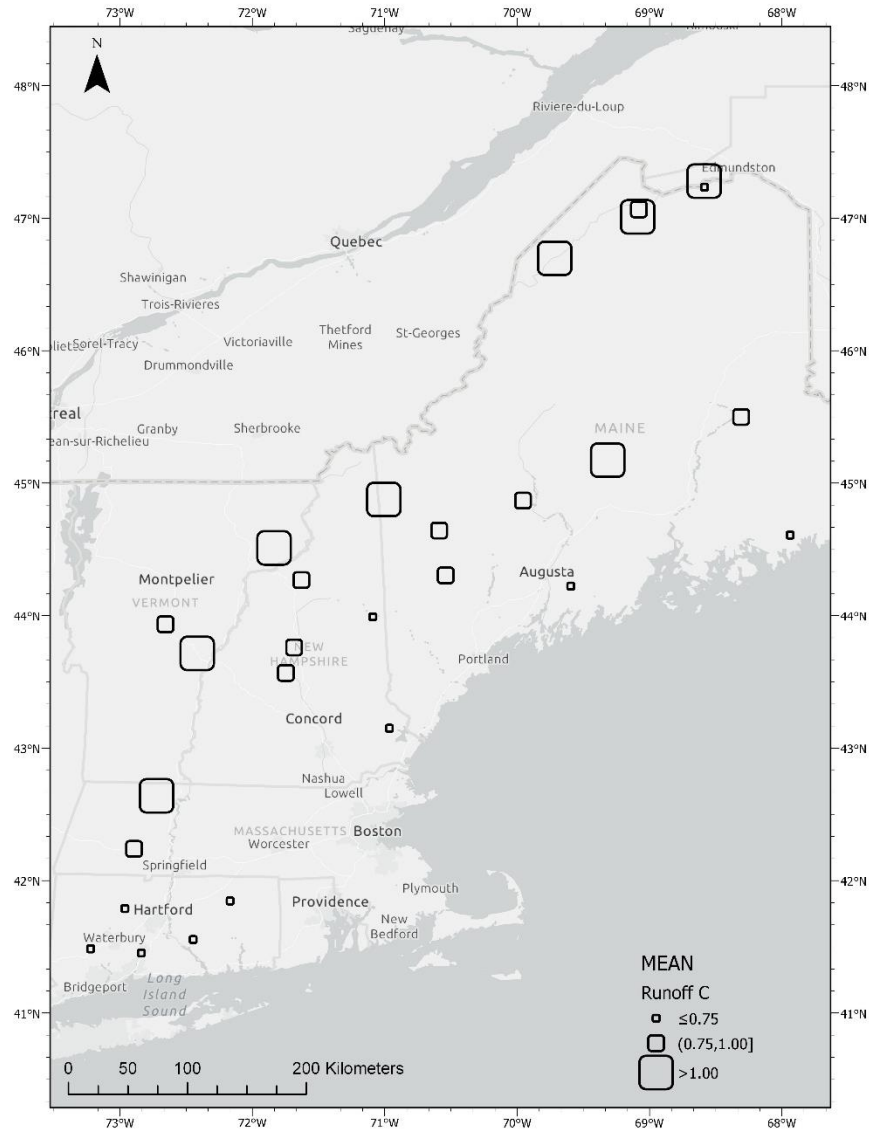


**Figure 4.** Average runoff coefficients of all high-flow events (2-year return period and greater) in 28 selected New England basins with natural flow conditions. Values were calculated using the base scenario.

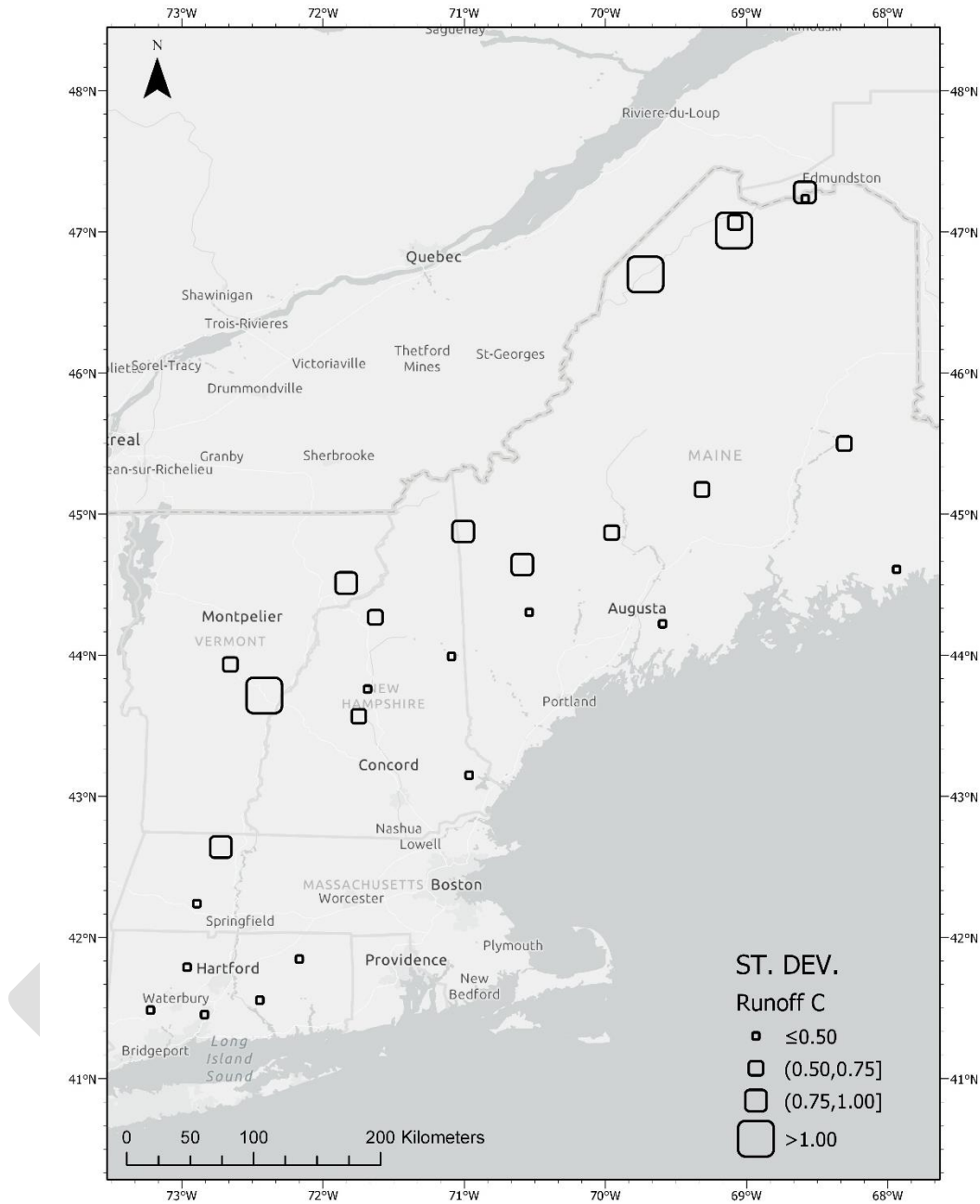


**Figure 5.** Standard deviation of runoff coefficients of all high-flow events (2-year return period and greater) in 28 selected New England basins with natural flow conditions. Values were calculated using the base scenario.



385 **Table 4.** Runoff coefficient (RC) statistics calculated using the base scenario for high-flow events from 1981 to 2016 in selected New  
 386 England basins

| No. | USGS Gage Station ID | USGS Gauge Station Name                      | State | RC Mean | RC Median | RC Standard Deviation | RC Max | Mann-Kendall S-value | Mann-Kendall p-value | Trend |
|-----|----------------------|--|-------|---------|-----------|-----------------------|--------|----------------------|----------------------|-------|
| 1   | 01010000             | St. John River at Ninemile Bridge            | ME    | 1.49    | 1.14      | 1.40                  | 6.86   | 58                   | 0.06                 | +     |
| 2   | 01010500             | St. John River at Dickey                     | ME    | 1.73    | 1.26      | 1.33                  | 6.52   | -14                  | 0.67                 | -     |
| 3   | 01011000             | Allagash River near Allagash                 | ME    | 0.85    | 0.74      | 0.58                  | 2.88   | -2                   | 0.98                 | -     |
| 4   | 01013500             | Fish River near Fort Kent                    | ME    | 0.61    | 0.58      | 0.41                  | 1.84   | -64                  | 0.04                 | -     |
| 5   | 01014000             | St. John River below Fish River at Fort Kent | ME    | 1.22    | 1.06      | 0.84                  | 3.73   | -14                  | 0.69                 | -     |
| 6   | 01022500             | Narraguagus River at Cherryfield             | ME    | 0.74    | 0.62      | 0.38                  | 1.72   | -90                  | 0.08                 | -     |
| 7   | 01030500             | Mattawamkeag River near Mattawamkeag         | ME    | 0.84    | 0.75      | 0.61                  | 2.58   | -11                  | 0.83                 | -     |
| 8   | 01031500             | Piscataquis River near Dover-Foxcroft        | ME    | 1.01    | 0.74      | 0.54                  | 2.36   | 39                   | 0.43                 | +     |
| 9   | 01038000             | Sheepscot River at North Whitefield          | ME    | 0.67    | 0.62      | 0.28                  | 1.35   | -22                  | 0.69                 | -     |
| 10  | 01047000             | Carrabassett River near North Anson          | ME    | 0.86    | 0.68      | 0.58                  | 3.16   | 18                   | 0.74                 | +     |
| 11  | 01052500             | Diamond River near Wentworth Location        | NH    | 2.12    | 2.11      | 0.97                  | 3.90   | -22                  | 0.34                 | -     |
| 12  | 01055000             | Swift River near Roxbury                     | ME    | 1.00    | 0.73      | 0.85                  | 3.74   | 9                    | 0.76                 | +     |
| 13  | 01057000             | Little Androscoggin River near South Paris   | ME    | 0.78    | 0.65      | 0.35                  | 1.47   | -12                  | 0.74                 | -     |
| 14  | 01064500             | Saco River near Conway                       | NH    | 0.64    | 0.62      | 0.21                  | 1.03   | 0                    | 1.00                 | -     |
| 15  | 01073000             | Oyster River near Durham                     | NH    | 0.70    | 0.68      | 0.19                  | 1.25   | 46                   | 0.26                 | +     |
| 16  | 01076500             | Pemigewasset River at Plymouth               | NH    | 0.90    | 0.69      | 0.47                  | 2.32   | -66                  | 0.13                 | -     |
| 17  | 01078000             | Smith River near Bristol                     | NH    | 0.86    | 0.62      | 0.67                  | 3.40   | -10                  | 0.87                 | -     |
| 18  | 01121000             | Mount Hope River near Warrenville            | CT    | 0.67    | 0.61      | 0.26                  | 1.42   | -40                  | 0.36                 | -     |
| 19  | 01134500             | Moose River at Victory                       | VT    | 1.48    | 1.34      | 0.97                  | 3.58   | -43                  | 0.24                 | -     |
| 20  | 01137500             | Ammonoosuc River at Bethlehem Junction       | NH    | 0.83    | 0.61      | 0.58                  | 3.06   | -2                   | 0.98                 | -     |
| 21  | 01142500             | Ayers Brook at Randolph                      | VT    | 0.96    | 0.83      | 0.63                  | 2.50   | -5                   | 0.91                 | -     |
| 22  | 01144000             | White River at West Hartford                 | VT    | 1.22    | 0.90      | 1.08                  | 4.16   | 6                    | 0.88                 | +     |
| 23  | 01169000             | North River at Shattuckville                 | MA    | 1.01    | 0.82      | 0.81                  | 4.25   | -70                  | 0.20                 | -     |
| 24  | 01181000             | West Branch Westfield River at Huntington    | MA    | 0.84    | 0.71      | 0.36                  | 2.10   | 78                   | 0.15                 | +     |
| 25  | 01188000             | Burlington Brook near Burlington             | CT    | 0.66    | 0.64      | 0.22                  | 1.20   | -30                  | 0.50                 | -     |
| 26  | 01193500             | Salmon River near East Hampton               | CT    | 0.68    | 0.65      | 0.21                  | 1.17   | 0                    | 1.00                 | -     |
| 27  | 01196500             | Quinnipiac River at Wallingford              | CT    | 0.53    | 0.52      | 0.13                  | 0.77   | -51                  | 0.46                 | -     |
| 28  | 01204000             | Pomperaug River at Southbury                 | CT    | 0.58    | 0.57      | 0.18                  | 0.92   | 47                   | 0.41                 | +     |

### 3.3 Temporal Trends

Daily precipitation above median (50% percentile) shows significant trends in 10 out of 28 basins (80% positive) during the period of record (1981–2016). Daily discharge above median shows trends in eight out of 28 basins (75% positive). The lack of substantial change in event discharge since 1980 is consistent with a previous analysis of the same gauges (Collins, 2009). Mann-Kendall trend analysis revealed that the RC of high-flow events was mainly stationary from 1981 to 2016. More specifically, the majority (89%) of study stations did not exhibit RC trends for high-flow events that were statistically significant at the 90% confidence level ( $\alpha=0.10$ ). Detailed results of the statistical analyses are presented in Table 4, which documents that only three out of 28 basins showed statistically significant trends (one positive and two negative trends) for the base scenario.

The lack of statistically significant trends in RCs did not depend on calculation alternatives. Increasing the high-flow event threshold to the 5-yr flood (scenario A2) did not result in statistically significant trends; increasing the high-flow event threshold to the 10-yr flood (scenario A3) did not result in enough events to draw statistical conclusions. Similarly, changes to the local minima duration (scenarios B1–B3) and to the baseflow separation method (scenarios C1–C4) did not result in statistically significant RC trends.

### 3.4 Seasonality of RC of High-flow Events

Seasonality analysis demonstrates the prevalence of the role of snowmelt in high-flow events in New England. Nineteen out of the 20 highest-RC events occurred in March or April (Table 3), which is the time of peak regional snowmelt. Moreover, 25 of the 28 drainage basins (89%) have their maximum RC in March and April.

The majority of high-flow events occurred in spring (64%) while the other 36% were distributed almost evenly in the rest of the year (Figure 6b). A preponderance of spring events has been previously observed in the Northeast U.S., both in New England as well as more southern basins that do not exhibit large snowpacks but do experience high seasonal soil moisture (Collins, 2019). Presumably as a result of the important effect of snowmelt in spring floods, the average RC of spring floods was 1.09 (Figure 6a). All other seasons exhibited RCs that were substantially lower (winter 0.65, autumn 0.55, and summer 0.53) over the period of analysis.

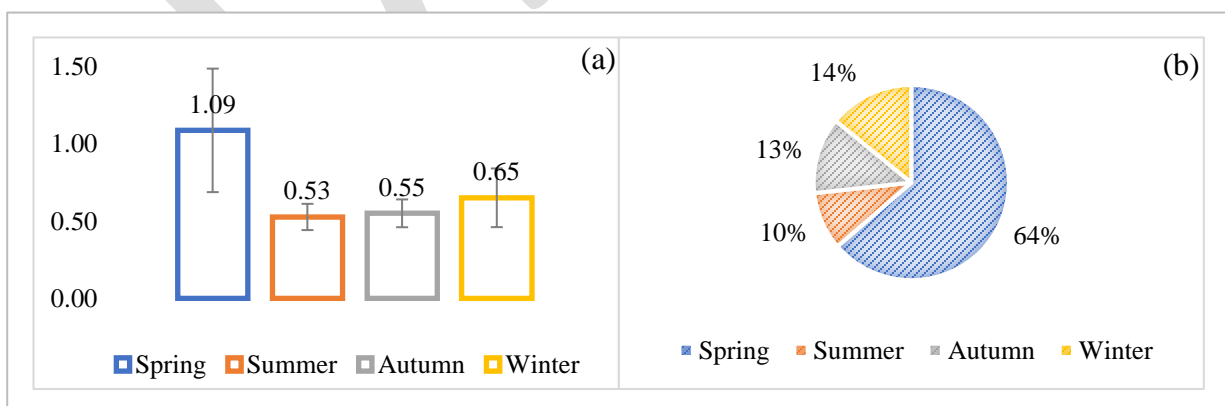


**Figure 6.** (a) Average runoff coefficient and (b) seasonal frequency of high-flow events in selected New England basins during spring (March, April, May), summer (June, July, August), autumn (September, October, November), and winter (December, January, February). Vertical bars represent one standard deviation

#### 4 Conclusions

Snow plays a major role in generating floods in New England. Runoff coefficients (RCs) in 28 undisturbed basins were found to be quite high, with many individual high-flow events creating RCs greater than 1.0, and the average high-flow RC exceeding 1.0 for 32% of study basins. Average RCs during high-flow events generally increased in magnitude and variability with distance from the coastline toward the north and west, accompanied by increases in altitude and latitude, and results were robust to various calculation alternatives. Overall, the majority (64%) of high-flow events occurred during the spring, and spring events exhibited the highest RC among all seasons (1.09). Previous work has suggested that snow in the Northeast U.S. generates floods through direct snow melt, rain-on-snow events, and increases in soil moisture (Collins et al., 2014), though these various mechanisms were not separated here.

Precipitation and runoff both increased in New England study basins in recent years (1981–2016), which is consistent with previous studies of the region (Hodgkins and Dudley, 2005; Wuebbles et al., 2017). However, increases were observed to offset each other, such that RCs for high-flow events were stationary. Proportional increases in precipitation and discharge dramatically simplify incorporating climatic changes into regional flood frequency management for infrastructure protection and water resources. For example, dam spillways are often rated for a particular flood recurrence interval (FEMA, 2015); being able to increase that flood level in direct proportion to recent or expected near-term future increases in future precipitation would enable the protection of public safety without requiring extensive basin-specific rainfall-runoff modeling. The presence of stationary RCs suggests that flood generation mechanisms within undisturbed basins have remained relatively stable within the region to date, perhaps because observed increases in precipitation have been counterbalanced by decreased snowpack storage or soil moisture content due to increasing temperature (Ivancic and Shaw, 2015). If so, the stationarity of RCs is likely only a temporary phenomenon.

Because snow plays such a large role in determining flood magnitudes, changes in snowfall and accumulation patterns will likely change RC magnitudes in the future. Future simulations of New England climate suggest that historical patterns of snowfall and accumulation are likely to change dramatically, with wintertime precipitation in New England shifting from being dominated by snow to rain, resulting in consequent decreases in the amount of snowpack and snowmelt (Easterling et al., 2017). Already, many sites within the northern U.S. are experiencing less consistent wintertime snow coverage, and snowpacks that do develop typically store less water than in the past (Burakowski et al., 2008).

As a result, understanding RCs in the future requires more in-depth hydrological modeling under different climate change scenarios that could incorporate flood-generation mechanisms and therefore explore expected changes in the frequency, magnitude, and timing of floods (e.g., Byun et al., 2019). Long-term infrastructure risk assessment and water resources management under a changing climate remains a challenge. In addition, this study only focused on undisturbed basins with natural flow so cannot be directly applied to flood prediction in basins with significant urbaniza-

tion, land use change, and/or dammed impoundments. The interplay between climate and landscape changes and the complexity of high-flow event generation adds additional uncertainty to forecasting future flood frequencies in New England.

## 5 Acknowledgments

The authors would like to thank Mathias Collins of the NOAA Office of Habitat Conservation for guidance and feedback during the progress of this study and for the review of a draft of this manuscript. Support for this project was provided by the National Science Foundation's Research Infrastructure Improvement NSF #IIA-1539071.

## References

- Armstrong, W.H., Collins, M.J., Snyder, N.P., 2014. Hydroclimatic flood trends in the northeastern United States and linkages with large-scale atmospheric circulation patterns. *Hydrol. Sci. J.* 59, 1636–1655. doi:10.1080/02626667.2013.862339
- Armstrong, W.H., Collins, M.J., Snyder, N.P., 2012. Increased Frequency of Low-Magnitude Floods in New England1. *JAWRA J. Am. Water Resour. Assoc.* 48, 306–320. doi:10.1111/j.1752-1688.2011.00613.x
- Arnell, N.W., Gosling, S.N., 2016. The impacts of climate change on river flood risk at the global scale. *Clim. Change.* doi:10.1007/s10584-014-1084-5
- Berghuijs, W.R., Woods, R.A., Hutton, C.J., Sivapalan, M., 2016. Dominant flood generating mechanisms across the United States. *Geophys. Res. Lett.* 43, 4382–4390. doi:10.1002/2016GL068070
- Burakowski, E.A., Wake, C.P., Braswell, B., Brown, D.P., 2008. Trends in wintertime climate in the northeastern United States: 1965–2005. *J. Geophys. Res.* 113, D20114. doi:10.1029/2008JD009870
- Byun, K., Chiu, C.M., Hamlet, A.F., 2019. Effects of 21st century climate change on seasonal flow regimes and hydrologic extremes over the Midwest and Great Lakes region of the US. *Sci. Total Environ.* 650, 1261–1277. doi:10.1016/j.scitotenv.2018.09.063
- Cleveland, W.S., 1979. Robust locally weighted regression and smoothing scatterplots. *J. Am. Stat. Assoc.* 74, 829–836. doi:10.1080/01621459.1979.10481038
- Collins, M.J., 2019. River flood seasonality in the Northeast United States: Characterization and trends. *Hydrol. Process.* 33, 687–698. doi:10.1002/hyp.13355
- Collins, M.J., 2009. Evidence for changing flood risk in New England since the late 20th century, *Journal of the American Water Resources Association.* doi:10.1111/j.1752-1688.2008.00277.x
- Collins, M.J., Kirk, J.P., Pettit, J., Degaetano, A.T., McCown, M.S., Peterson, T.C., Means, T.N., Zhang, X., 2014. Annual floods in new england (USA) and atlantic canada: Synoptic climatology and generating mechanisms. *Phys. Geogr.* 35, 195–219. doi:10.1080/02723646.2014.888510
- Colonell, J.M., Higgins, G.R., 1973. Hydrologic Response of Massachusetts Watersheds. *JAWRA J. Am. Water Resour. Assoc.* 9, 793–800. doi:10.1111/j.1752-1688.1973.tb01800.x

- 502 Demaria, E.M.C., Palmer, R.N., Roundy, J.K., 2016. Regional climate change projections of  
503 streamflow characteristics in the Northeast and Midwest U.S. *J. Hydrol. Reg. Stud.* 5, 309–  
504 323. doi:10.1016/j.ejrh.2015.11.007
- 505 Dingman, L.S., 2002. *Physical Hydrology*, Prentice Hall. Prentice Hall.
- 506 Easterling, D.R., Kunkel, K.E., Arnold, J.R., Knutson, T., LeGrande, A.N., Leung, L.R., Vose,  
507 R.S., Waliser, D.E., Wehner, M.F., 2017. Precipitation change in the United States. In:  
508 Climate Science Special Report: Fourth National Climate Assessment, Volume I [Wuebbles,  
509 D.J., D.W. Fahey, K.A. Hibbard, D.J. Dokken, B.C. Stewart, and T.K. Maycock (eds.)].  
510 doi:10.7930/J0H993CC
- 511 FEMA, 2015. Federal Guidelines for Dam Safety Risk Management.
- 512 Gilleland, E., Katz, R.W., 2016. extRemes 2.0: An Extreme Value Analysis Package in R. *J. Stat.*  
513 *Softw.* 72, 1–39. doi:10.18637/jss.v072.i08
- 514 Groisman, P.Y., Knight, R.W., Easterling, D.R., Karl, T.R., Hegerl, G.C., Razuvaev, V.N., 2005.  
515 Trends in intense precipitation in the climate record. *J. Clim.* 18, 1326–1350.  
516 doi:10.1175/JCLI3339.1
- 517 Groisman, P.Y., Knight, R.W., Karl, T.R., Easterling, D.R., Sun, B., Lawrimore, J.H., 2004.  
518 Contemporary Changes of the Hydrological Cycle over the Contiguous United States: Trends  
519 Derived from In Situ Observations. *J. Hydrometeorol.* 5, 64–85. doi:10.1175/1525-  
520 7541(2004)005<0064:CCOTHC>2.0.CO;2
- 521 Hansen, J., Ruedy, R., Sato, M., Lo, K., 2010. Global surface temperature change. *Rev. Geophys.*  
522 48.
- 523 Hewlett, J.D., Cunningham, G.B., Troendle, C.A., 1977. Predicting Stormflow and Peakflow from  
524 Small Basins in Humid Area by the R-index Method. *JAWRA J. Am. Water Resour. Assoc.*  
525 13, 231–254. doi:10.1111/j.1752-1688.1977.tb02021.x
- 526 Hipel, K.W., McLeod, A.I., 1994. *Time series modelling of water resources and environmental*  
527 *systems*. Elsevier.
- 528 Hirsch, R.M., Archfield, S.A., 2015. Flood trends: Not higher but more often. *Nat. Clim. Chang.*  
529 5, 198–199. doi:10.1038/nclimate2551
- 530 Hodgkins, G.A., Dudley, R.W., 2005. Changes in the Magnitude of Annual and Monthly  
531 Streamflows in New England, 1902-2002. USGS Scientific Investigations Report 2005-5135.  
532 Reston, Virginia.
- 533 Ivancic, T.J., Shaw, S.B., 2015. Examining why trends in very heavy precipitation should not be  
534 mistaken for trends in very high river discharge. *Clim. Change* 133, 681–693.  
535 doi:10.1007/s10584-015-1476-1
- 536 Karl, T.R., Knight, R.W., 1998. Secular trends of precipitation amount, frequency, and intensity  
537 in the United States. *Bull. Am. Meteorol. Soc.* 79, 2552–2554.
- 538 Lins, H.F., Slack, J.R., 2005. Seasonal and Regional Characteristics of U.S. Streamflow Trends in  
539 the United States from 1940 to 1999. *Phys. Geogr.* 26, 489–501. doi:10.2747/0272-

- 540 3646.26.6.489
- 541 Madsen, T., Figdor, E., 2007. When it Rains it Pours, Environment America Research & Policy  
542 Center. doi:10.1177/01461672992512010
- 543 Mallakpour, I., Villarini, G., 2017. Analysis of changes in the magnitude, frequency, and  
544 seasonality of heavy precipitation over the contiguous USA. *Theor. Appl. Climatol.* 130, 345–  
545 363. doi:10.1007/s00704-016-1881-z
- 546 Matthews, J.H., Wickel, B.A.J., Freeman, S., 2011. Converging Currents in Climate-Relevant  
547 Conservation: Water, Infrastructure, and Institutions. *PLoS Biol.* 9, e1001159.  
548 doi:10.1371/journal.pbio.1001159
- 549 McCabe, G.J., Wolock, D.M., 2002. A step increase in streamflow in the conterminous United  
550 States. *Geophys. Res. Lett.* 29, 38-1-38-4. doi:10.1029/2002GL015999
- 551 McLeod, A.I., 2011. Kendall: Kendall rank correlation and Mann-Kendall trend test.
- 552 National Weather Service, 2018. Weather Related Fatality and Injury Statistics [WWW  
553 Document]. URL <https://www.weather.gov/hazstat/> (accessed 12.10.19).
- 554 Paulson, R., Chase, E., Roberts, R., Moody, D., 1991. National water summary 1988-89:  
555 Hydrologic events and floods and droughts, Water Supply Paper. doi:10.3133/wsp2375
- 556 PRISM Climate Group, 2004. PRISM Gridded Climate Data [WWW Document]. Oregon State  
557 Univ. URL <http://prism.oregonstate.edu/>
- 558 Prosdociimi, I., Kjeldsen, T.R., Miller, J.D., 2015. Detection and attribution of urbanization effect  
559 on flood extremes using nonstationary flood-frequency models. *Water Resour. Res.* 51, 4244–  
560 4262. doi:10.1002/2015WR017065.Received
- 561 R Core Team, 2019. R: A language and environment for statistical computing.
- 562 Reusser, D., Buytaert, W., Vitolo, C., 2017. RHydro: Classes and methods for hydrological  
563 modelling and analysis.
- 564 Ryberg, K.R., Vecchia, A. V., 2017. waterData: Retrieval, Analysis, and Anomaly Calculation of  
565 Daily Hydrologic Time Series Data.
- 566 Satterthwaite, D., 2008. Climate Change and Urbanisation: Effects and Implications for Urban  
567 Governance - GSDRC.
- 568 Slater, L.J., Villarini, G., 2016. Recent trends in U.S. flood risk. *Geophys. Res. Lett.* 43, 12,428-  
569 12,436. doi:10.1002/2016GL071199
- 570 Small, D., Islam, S., Vogel, R.M., 2006. Trends in precipitation and streamflow in the eastern U.S.:  
571 Paradox or perception? *Geophys. Res. Lett.* 33, 2–5. doi:10.1029/2005GL024995
- 572 Smith, A., Lott, N., Houston, T., Shein, K., Crouch, J., Enloe, J., 2019. U.S. Billion-Dollar Weather  
573 Climate Disasters 1980-2019.
- 574 Spierre, S.G., Wake, C., Gittell, R., Carter, J.R., Kelly, T., Schaefer, D., 2010. Trends in Extreme  
575 Precipitation Events for the Northeastern United States. Durham, NH.

- 576 USGS, 2019. USGS Water Data for the Nation [WWW Document]. Natl. Water Inf. Syst. Web  
577 Interface. doi:10.5066/F7P55KJN
- 578 USGS, 2017. StreamStats, Version 4, Fact Sheet 2017–3046. doi:10.3133/fs20173046
- 579 Woldemeskel, F., Sharma, A., 2016. Should flood regimes change in a warming climate? The role  
580 of antecedent moisture conditions. *Geophys. Res. Lett.* 43, 7556–7563.  
581 doi:10.1002/2016GL069448
- 582 Woodruff, J.F., Hewlett, J.D., 1970. Predicting and Mapping the Average Hydrologic Response  
583 for the Eastern United States. *Water Resour. Res.* 6, 1312–1326.  
584 doi:10.1029/WR006i005p01312
- 585 Wuebbles, D.J., Fahey, D.W., Hibbard, K.A., Dokken, D.J., Stewart, B.C., Maycock, T.K., 2017.  
586 Climate science special report: fourth National Climate Assessment, U.S. Global Change  
587 Research Program. doi:10.7930/J0J964J6
- 588